Revision 1

# Ti resetting in quartz during dynamic recrystallization: Mechanisms and significance

**Kyle T. Ashley[1,*], William D. Carlson[2], Richard D. Law[1], and Robert J. Tracy[1]**

[1]Department of Geosciences, Virginia Tech, 4044 Derring Hall (0420), Blacksburg, VA 24060, USA

[2]Department of Geological Sciences, University of Texas at Austin, 2275 Speedway Stop C9000, Austin, TX 78712, USA

[*]Corresponding author: Tel. +1 315 244 5546; E-mail: ktashley@vt.edu

*Running title:* Ti resetting in quartz during dynamic recrystallization

# Ti resetting in quartz during dynamic recrystallization: Mechanisms and significance

## ABSTRACT

The ubiquity of quartz in continental crust, and the involvement of $SiO_2$ in multiple metamorphic processes such as reactions, fluid flux, and solution-transfer processes, makes quartz an obvious choice for reconstructing prograde metamorphic conditions in a variety of rock types. Recent studies have shown the usefulness of analyzing Ti distribution in quartz to constrain pressure - temperature - (relative) time - deformation (*P-T-t-D*) in metamorphosed tectonites. New high-precision single crystal X-ray diffraction volume constraints on Ti-doped and chemically pure quartz provide further evidence for substitution of $Ti^{4+}$ for $Si^{4+}$ in the tetrahedral site in quartz, with resultant lattice strain on the structure.

Recent applications of the Ti-in-quartz thermobarometer to dynamically recrystallized quartz have identified recrystallized subgrains that contain lower Ti concentrations ([Ti]) than their host porphyroclasts. In addition, [Ti] are lower than expected for the temperatures of recrystallization. Atomistic simulations that estimate energetic perturbations resulting from Ti incorporation into the quartz lattice indicate that significant increases in strain energy occur only at very high [Ti]; the strain-energy increase is negligible for [Ti] typical of quartz grown under mid-crustal conditions. This suggests that lattice strain rarely provides an appreciable driving force for Ti loss from quartz; instead, it appears that subgrain boundaries and dislocation arrays migrating through recrystallizing quartz crystals can promote localized re-equilibration, thermodynamically regulated by the composition of the intergranular medium (typically undersaturated in Ti). It therefore appears that analyses from dynamically recrystallized quartz

cannot be meaningfully interpreted until methods are developed that can account quantitatively for the reduction of Ti resulting from crystal plastic flow.

**Keywords:** Titanium, quartz, dynamic recrystallization, lattice strain, atomistic simulation

## INTRODUCTION

Thermobarometry is of key importance in metamorphic and structural petrology for reconstructing the pressure-temperature-deformation (*P-T-D*) histories of metamorphic tectonites and the geologic evolution of orogenic terranes. Peak metamorphism is often considered because equilibration is most prominent at peak temperature and speaks most directly to the depth the rocks reached and the mechanisms for burial and exhumation. Tectonic models are derived from *P-T* profiles with respect to structural transects to explain the evolution of the tectonic environment. The Ti-in-quartz ("TitaniQ") thermobarometer has been applied to a wide variety of rocks in various tectonic environments since its initial calibration by Wark and Watson (2006). Applied to pelitic schists metamorphosed at mid-crustal depths, the TitaniQ thermobarometer has been shown to be an effective monitor of Si-flux resulting from: (i) metamorphic reactions, (ii) strain-induced solution transfer, and (iii) Si-charged fluid influx (Ashley et al., 2013). The commonality among these three re-equilibration scenarios is that they are all the result of quartz growth events. In no cases studied by Ashley et al. (2013) were peak-*T* conditions preserved. This is because of the low diffusivity of Ti in quartz under typical Barrovian metamorphic conditions and the inability of Ti in the quartz lattice to re-equilibrate at tectonically significant time scales under the *PT* conditions studied. Recent attempts have been aimed at interpreting results from deformed quartzites. However, dynamically recrystallized quartz has concentrations of Ti ([Ti]) much lower than expected for the temperatures required to activate dislocation slip systems for the inferred recrystallization regimes (e.g., Grujic et al., 2011; Ashley et al., 2013; Nachlas et al., 2013). In this article, we discuss: (i) potential mechanisms to drive quartz re-equilibration with respect to Ti (growth *vs.* recrystallization); (ii) crystallographic and energetic consequences resulting from Ti substitution for Si, including

atomistic simulation to evaluate interactions among Ti defects; and (iii) the effect of dynamic recrystallization on Ti solubility in quartz. Insights gained from application of the TitaniQ thermobarometer to quartz mylonites by various research groups are discussed to help guide future applications of the TitaniQ thermobarometer in geologically appropriate scenarios.

## TITANIUM INCORPORATION IN QUARTZ

### Crystallographic incorporation

The incorporation of $Ti^{4+}$ into quartz has previously been attributed to isomorphic and isoelectronic substitution for the $Si^{4+}$ ion, with significant temperature and, to a lesser extent, pressure, influences (e.g., Müller et al., 2003). Numerous experiments, including X-ray absorption near-edge structure (XANES) and density functional theory (DFT) calculations, support the tetrahedral incorporation of $Ti^{4+}$, with no evidence for octahedral coordination (Thomas et al., 2010, and references therein). The stereochemistry of $Si^{4+}$ in the tetrahedral sites is controlled by ~50/50 ionic-covalent bonding with oxygen (determined through electronegativity, electron-density calculations, and valence-bond structuring; Pauling, 1980), forming four molecular hybrid orbitals ($sp^3$) that are arranged in a regular tetrahedral form to minimize electron repulsion. Ionic modeling of the substitution alone cannot explain this exchange, because $Ti^{4+}$ ions may not be of appropriate size. However, a bonding-orbital (covalent) model could explain this substitution because the electronic configurations of $Ti^{4+}$ (with zero *3d* electrons) would result in no crystal field stabilization energy resulting between the transition metal and the ligands (Burns, 1970), and would minimize lattice energies, except for strain energy, with this coordination. Ti may also be present in quartz as nano-inclusions or mineral precipitates; in that case, however, six-fold coordination is expected, as in rutile,

brookite, or possibly more exotic alkali oxides (e.g., $Li_4TiO_4$, Gunawardane et al., 1994). It is important to determine unequivocally the dominant incorporation mechanisms of Ti in quartz because the most appropriate functional form of the thermodynamic equations used to describe the temperature dependence is different for different mechanisms: precipitate-based incorporation is better described by an Arrhenian temperature-dependence equation (with a diffusion coefficient), rather than the configurational entropy mixing term used for substitution in the lattice. For example, in the case of non-lattice structural substitution, pressure and temperature would strongly affect precipitate densities and could yield the [Ti] correlation previously described in the literature (e.g. Wark and Watson, 2006; Thomas et al., 2010).

**Volume XRD measurements**

The hydrothermal experimentation technique used to grow quartz at *P* and *T* conditions of interest in Thomas et al. (2010) relies on quenching the sample to preserve Ti atoms in their incorporated crystallographic sites. Absolute X-ray diffraction (XRD) volumetric measurements are warranted here for samples prepared in this manner, because elastic properties are not quenchable and regress to ambient values after the experiment is finished (Raz et al., 2002). Ti present as rutile nanoinclusions or precipitates would be expected to induce some degree of lattice strain, but should not expand the lattice volume. Any observable volume increase may be an indication that Ti substitutes for Si in the tetrahedral site.

Single-crystal X-ray diffraction measurements were conducted on a customized Huber four-circle goniometer diffractometer fitted with an unfiltered Mo sealed-tube X-ray source (without a monochromator). Measurements are made with a fixed-$\varphi$ mode and driven 0.001° per

motor step for $\omega$ and $\chi$. For a complete description of the experimental set-up and instrumentation conditions used, see Angel et al. (1997).

The diffractometer was driven by the program SINGLE (Angel et al., 2000), which uses vector-least-squares refinement of unit-cell parameters and 8-position peak-centering algorithms (described by Angel et al., 1997) to produce extremely high-precision measurements. Lattice refinements on a synthetic high-Ti sample from Thomas et al. (2010) (QTip-38, *ca.* 380 ppm Ti) and on a chemically pure crystal were completed to determine if volume perturbation with Ti substitution exists. Both crystals were untwinned and nearly spherical. The resultant refined lattice volumes are 113.0180(40) $Å^3$ and 113.1342(236) $Å^3$ for the chemically-pure standard and Ti-doped crystal, respectively; this difference is statistically significant at the 95% confidence level.

## MECHANISMS FOR TI REDISTRIBUTION

Due to multiple re-equilibrating drivers active during dynamic recrystallization of quartz (e.g., chemical thermodynamics, strain-minimizing dislocation creep systems, etc.), understanding the dominant factor controlling Ti redistribution is important for thermobarometric calibrations. Here we examine two mechanisms for loss of Ti from the quartz lattice during recrystallization, which differ importantly in terms of the principal driving force for Ti loss.

### Mechanism 1: Strain-driven relocation of Ti

Substitution of Ti into a Si site in quartz will induce strain on the structure; the strain energy increases non-linearly with Ti concentration, because Ti atoms in close proximity yield greater total strain than Ti atoms far from one another. Such structural strain is thus an energetic driver for Ti atoms in quartz to migrate to positions with maximum separation. If an appropriate path for fast diffusion is made available (e.g., as a grain boundary sweeps through the crystal), then movement of Ti ions completely out of the quartz grain and into the intergranular medium or a subgrain boundary is expected to decrease the energy of the quartz structure. However, for this mechanism to be a primary driver for Ti redistribution in quartz undergoing crystal plastic flow, the energy perturbation resulting from the removal must be appreciable at [Ti] observed in natural settings. That is, if removing a Ti atom from a quartz crystal results in a negligible decrease in strain energy, this mechanism may be insufficient to drive Ti mobility.

### Mechanism 2: Localized thermodynamic control from intergranular medium

An alternative mechanism for Ti loss during deformation is local re-equilibration within a microenvironment where the intergranular medium constitutes the subgrain boundary. Fluids present in this region would control the effective concentration of $TiO_2$, where the $TiO_2$ activity is most likely below unity (i.e., not rutile-saturated). In this scenario, chemical-potential differences would be the dominant driving force for Ti loss from quartz and would result in [Ti] much lower than expected when assuming an activity close to 1 (typically valid for metapelites; Ghent and Stout, 1984).

## ATOMISTIC SIMULATION OF INTERACTIONS AMONG TI DEFECTS

Atomistic simulation provides a means of estimating the magnitude of the increases in strain energy due to interactions of Ti defects at varying levels of concentration. Such calculations help to discriminate between the two mechanisms described above, by identifying concentration levels below which the defects are sufficiently far apart that further reduction in concentration has only a negligible effect on the lattice energy.

These simulations use interatomic potentials based on an ionic model with formal integral charges. Short-range interactions for $Si^{4+}$–$O^{2-}$, $Ti^{4+}$–$O^{2-}$, and $O^{2-}$–$O^{2-}$ are described by two-body Buckingham potentials, for which the potential ($U$) for ions separated by distance $r$ is given by $U(r) = A \cdot \exp(-r/\rho) - (C/r^6)$. O-Si-O bending terms have the form $U(\theta) = \frac{1}{2} K_B (\theta - \theta_0)^2$. Oxygen-ion polarizability (shell model of Dick and Overhauser, 1958) is included via a core-shell interaction potential at separation $r$ of the form $U(r) = \frac{1}{2} k r^2$. We note that although the potential set used by Lewis and Catlow (1986) included polarizability for Ti, the effect is negligibly small and is therefore omitted in this work. Cation-cation interactions beyond electrostatics are neglected. Values for potential parameters and their sources are given in Table 1. This potential set was shown by Sanders et al. (1984) to successfully reproduce the known properties of $SiO_2$ polymorphs, including α-quartz as modeled here.

All simulations were performed using GULP, the General Utility Lattice Program (Gale, 1997; Gale and Rohl, 2003). Calculations were done in the static limit ($T$ = 0 K, $P$ = 0 GPa). Defect energies in this limit approximate corresponding defect enthalpies at elevated temperatures to within a few percent (Taylor et al., 1997), and defect free energies in silicates (garnet) have been shown to change very little across a wide range of geologic temperatures and pressures (Carlson et al., 2014). Lattice energies were computed for supercells containing a single Ti atom in place of Si, relaxing the structure to its minimum energy state. Sizes of

supercells were progressively increased to evaluate the energy variance with decreasing [Ti], and increasing Ti-Ti distance (Table 2). The energy due to defect interactions drops off sharply with increased Ti-Ti spacing (Fig. 1), and is negligible at separation distances > ~30 Å, which corresponds to < 1000 ppm Ti. To validate this result, the energy of a single isolated defect (Ti in limit of infinite dilution) was evaluated using the embedded-cluster method and the two-region Mott-Littleton approach (Mott and Littleton, 1938), with region sizes progressively enlarged until energy convergence was achieved (region 1 radius = 18 Å (3397 atoms); region 2 radius = 24 Å (4688 atoms)). The energy calculated in this way for an isolated defect is indistinguishable from the defect energy for a 9x9x9 supercell, confirming the inference that interactions between Ti defects are energetically negligible once [Ti] drops below ~1000 ppm.

## DISCUSSION

Titanium distribution in quartz can be qualitatively evaluated using cathodoluminescence (CL) imaging through blue filtration, due to the proportionality of Ti concentration to the resultant CL emission (Wark and Spear, 2005; Rusk et al., 2006; Rusk et al., 2008; Spear and Wark, 2009). Zoning patterns in individual grains can be interpreted with respect to pressure-temperature-growth histories (Spear and Wark, 2009; Ashley et al., 2013), whereas distribution analysis of a population of grains can be interpreted in the context of deformation histories.

Here we will evaluate the results from a compilation of various studies in which Ti-in-quartz thermometry was applied to dynamically recrystallized quartz in shear zones to obtain temperatures of deformation. Our intent is to make a global evaluation of mechanisms driving Ti re-equilibration, rather than focusing on results from one field site.

## Experimentally deformed Ti-doped quartz aggregates

Investigating the effects that crystal plastic flow has on Ti redistribution is difficult due to the large number of variables that may perturb the system. For a quartz mylonite, for example, water weakening, strain rate, grain size, temperature, and other factors all influence crystal mechanics. From a thermodynamic perspective, starting aggregate heterogeneity, $TiO_2$ activity, diffusion, and the presence of fluids on defects and grain boundaries further complicate this assessment. Many of these variables are difficult to constrain accurately in natural settings, and cross-term effects may obscure some intrinsic trends. Nachlas et al. (2013) conducted dynamic deformation experiments at constant *P* and *T* in a shear-assembly apparatus for various strain rates. They developed an innovative doping technique to prepare homogenized quartz aggregates of known starting [Ti]. These experiments evaluated the influence of constrainable variables (starting [Ti], strain rate, water content, duration, etc.) on grain size, resultant recrystallized grain [Ti], and subgrain heterogeneity. Newly formed recrystallized grains typically have [Ti] much lower than expected when using the Thomas et al. (2010) calibration for the experimental conditions. More importantly, Nachlas et al. (2013) recognized the impact of duration of dynamic recrystallization for resultant trace element composition, and acknowledged the significance of kinetics and diffusion on Ti redistribution.

## [Ti] in recrystallized quartz subgrains in natural systems

Recent applications of the TitaniQ thermobarometer have pursued the effects of crystal plastic flow on Ti resetting. The findings from Ashley et al. (2013), Grujic et al. (2011) and Kidder et al. (2013) are discussed to provide a natural context for interpreting the data presented

in this study. In each investigation, recrystallized subgrains contained [Ti] lower than that of their host porphyroclastic cores (Fig. 2).

The study by Ashley et al. (2013) emphasized the utility of the TitaniQ thermobarometer in constraining *P-T-D* histories and monitoring Si-flux in metapelitic tectonites. The results presented in that study are in good agreement with previous petrologic estimates on the same rocks. The abundant biotite present in their samples acts as a weak interconnected phase that accommodates strain in the rock, with dynamically recrystallized quartz being largely absent as a result. Two generations of quartz veining were observed in the Ashley et al. (2013) investigation: undeformed retrograde veins, and pre- or syn-kinematic veins that are extensively recrystallized by subgrain rotation recrystallization. Ti-in-quartz thermometry on recrystallized grains result in temperature estimates lower than expected from the inferred recrystallization mechanisms. This is an interesting observation, considering that undeformed quartz in these rocks yields expected temperatures, suggesting that dynamic recrystallization had a significant impact on the resultant [Ti] present in grains. Ashley et al. did not interpret the analytical results from these deformed quartz veins due to this discrepancy.

The Tonale mylonites studied by Grujic et al. (2011) have been extensively investigated and this locality is often used as a natural laboratory for petrologic and fabric studies. Despite a well-constrained *P-T* framework, many of the recrystallized quartz grains contain [Ti] much lower than expected from syn-deformation metamorphic mineral assemblages when using the Thomas et al. (2010) calibration. Decreasing the $TiO_2$ activity to *ca.* 0.2 results in temperature estimates that agree reasonably well with previous petrologic studies, but in the subgrain-rotation recrystallization regime, calculated temperatures are still much lower than indicated by metamorphic mineral assemblages. Although Grujic et al. acknowledge that it is unclear why the

243 $TiO_2$ activities in quartz mylonites would be so low, they attribute this discrepancy to: (i)
244 recrystallization influencing the activity (or resulting in an apparent activity) and, (ii) the
245 importance of a Ti-phase that may be recrystallizing or participating in a metamorphic reaction
246 that is synchronous with quartz recrystallization (an observation also discussed by Thomas,
247 2013). Considering the effects of recrystallization on the apparent $TiO_2$ activity explains why
248 adjusting the activity may work for some regimes (e.g., dynamic recrystallization) but does not
249 extrapolate into other regimes (e.g., subgrain rotation recrystallization). This is to be expected
250 because different recrystallization regimes may have different mechanisms operating to
251 minimize intracrystalline strain. For example, subgrain rotation recrystallization may have
252 dominant rhomb and prismatic slip to homogenize dislocation densities (Blacic, 1975), whereas
253 grain boundary bulging recrystallization may be dominated by basal slip (Hirth and Tullis,
254 1992).

255 Kidder et al. (2013) suggested two important factors should be considered when
256 analyzing [Ti] in recrystallized quartz: (i) the duration of deformation may have a significant
257 impact on Ti resetting due to diffusional limits (also acknowledged by Nachlas et al., 2013, in
258 the experimental deformation studies discussed above); and (ii) the importance of deviation of
259 fluid pressure from lithostatic pressure. The equivalence of fluid and lithostatic pressure is often
260 assumed, and in many systems may be appropriate (e.g., magmas, mid-to-deep crustal
261 metamorphism, very dry rocks). However, in systems where the fluid pressure deviates greatly
262 from lithostatic pressure (e.g., shallow quartz veins), this difference could have a significant
263 impact on the solubility of Ti in quartz and may result in erroneous estimated temperatures.
264

265 **Lattice energetics with Ti substitution**

The XRD measurements conducted in this study reflect structural adjustments that result from substituting Ti for Si on tetrahedral sites. The observed (mean) volume difference can be attributed to differences in [Ti] because all other conditions (e.g., analytical conditions, crystal morphology, absence of twins) are identical. A larger unit cell volume is measured for the Ti-doped quartz, suggesting that substituting the larger Ti cation for Si results in an expanded lattice. The larger uncertainty for the measured volume of the Ti-doped crystal is likewise attributed to lattice strain resulting from the substitution of Ti for Si.

Our atomistic simulations illustrate the energy consequences of substituting Ti in quartz for a range of concentrations. Quartz grown under typical Barrovian metamorphic conditions contains [Ti] in the 10s of ppm or less. At these concentrations, there would be a negligible increase in lattice energy relative to a pristine crystal (Fig. 1). This suggests that the amount of lattice strain resulting from typical levels of Ti substitution is not sufficient to drive significant Ti redistribution. Therefore, localized thermodynamic factors must provide the dominant driving force for removing Ti from quartz.

Diffusion rates for Ti in quartz at temperatures < 600 °C are sluggish (Cherniak et al., 2007), and the duration of deformation in tectonic systems may be too short to expect complete equilibration of the recrystallized subgrains. For example, deformation is believed to have occurred in < 1 Myr for the Tonale mylonites (Grujic et al., 2011). At the temperatures reported for subgrain rotation recrystallization in that study, the maximum distance of diffusion is < 10 μm. The process of sweeping grain boundaries and dislocations through the crystals during dynamic recrystallization provides short pathways for Ti diffusion. This intergranular medium would regulate the thermodynamics of this re-equilibration, and any fluids present would likely be far removed from $TiO_2$ saturation. Unlike new quartz growth, for which activity is driven by a

289 larger effective ("bulk rock") composition (controlled by local mineral content in a
290 microstructural domain), the effective composition regulating Ti partitioning during dynamic
291 recrystallization is of a much smaller volume (< 10 radial microns). Therefore
292 thermodynamically controlled re-equilibration would result in the removal of Ti from the lattice,
293 aided by the short diffusive pathways when migrating dislocations and subgrain boundaries are
294 present.
295

296 ## IMPLICATIONS

297 Proper recognition of the mechanisms for Ti re-equilibration in quartz is essential to
298 minimize the potential for erroneous temperature or pressure estimates. We question the
299 interpretation of measurements from extensively recrystallized quartz by means of calibrations
300 that were derived from growth experiments (e.g., Thomas et al., 2010; Huang and Audétat,
301 2012). Previous studies acknowledged the importance of starting heterogeneity in the deforming
302 quartz aggregate and duration of deformation on equilibrating subgrains. This study adds to these
303 observations by noting the importance of sweeping grain boundaries and defects through the
304 crystals to establish $TiO_2$-undersaturated thermodynamic "microenvironments" that drive
305 diffusion of Ti out of the crystal structure. Although the strain-energy increase produced by the
306 substitution of Ti for Si on tetrahedral sites in quartz is likely to be energetically unimportant in
307 typical Barrovian-sequence rocks, high-Ti quartz in other systems may have a significant energy
308 driver for redistributing Ti. Future work should focus on a calibration that takes into
309 consideration the dynamic recrystallization regime, duration of deformation, and greatly reduced
310 $TiO_2$ activities. This would serve as a more appropriate expression to infer temperatures of
311 deformation.

Considering the current state of the Ti-in-quartz thermobarometer, the following protocols are recommended to ensure appropriate usage:

1. CL imaging of quartz should always be conducted to prevent erroneous interpretations that may arise from assuming homogenized Ti distributions that are not actually present.

2. In instances where there is evidence for quartz growth (e.g., via quartz-producing metamorphic reactions, strain-induced solution transfer, Si-influx), the Thomas et al. (2010) calibration should be used. This may only be warranted in systems where pore fluid pressure is equal to the lithostatic pressure (e.g., application to mid-crustal rocks); in other circumstances, the Huang and Audétat (2012) calibration may be preferred.

3. Interpreting Ti-in-quartz data from dynamically recrystallized quartz should be done with caution or avoided until a calibration is developed that considers the mechanisms driving re-equilibration on these localized scales, along with the duration of recrystallization. It is likely that [Ti] in recrystallized quartz will yield spuriously low temperatures if the Thomas et al. (2010) calibration is used, and applying calibrations that result in higher *T* estimates for these conditions (e.g., Huang and Audétat, 2012) may also be erroneous.

4. When estimating temperatures from vein quartz, $TiO_2$ activity should be carefully considered, in recognition that veins free of Ti-saturated phases are common, and within such veins, restricted equilibration with the surrounding host rock may preclude rutile saturation.

## ACKNOWLEDGEMENTS

We are very grateful for the assistance of John Hughes, Elinor Spencer, Jing Zhao and Nancy Ross in the collection of X-ray diffraction analyses. We thank John Hughes for his review of this manuscript and Oliver Tschauner for editorial handling. This paper is based on work supported by the National Science Foundation under grant No. EAR-1220345 (awarded to R.D. Law) and by a Grant-In-Aid of Research from Sigma Xi, The Scientific Research Society (awarded to K.T. Ashley). The Texas Advanced Computing Center (TACC) at the University of Texas at Austin provided high-performance computing resources used for atomistic simulation.

340 ## REFERENCES

341 Angel, R.J., Allan, D.R., Miletich, R., and Finger, L.W. (1997) The use of quartz as an internal
342 pressure standard in high-pressure crystallography. Journal of Applied Crystallography,
343 30, 461-466.
344 Angel, R.J., Downs, R., and Finger, L.W. (2000) High-temperature-high-pressure diffractometry.
345 In R.M. Hazen, and R. Downs, Eds. High-Temperature and High-Pressure Crystal
346 Chemistry, 41, p. 559-596. Reviews in Mineralogy and Geochemistry, Washington, DC.
347 Ashley, K.T., Webb, L.E., Spear, F.S., and Thomas, J.B. (2013) *P-T-D* histories from quartz: A
348 case study of the application of the TitaniQ thermobarometer to progressive fabric
349 development in metapelites. Geochemistry Geophysics Geosystems, 14(9), 3821-3843.
350 Blacic, J.D. (1975) Plastic deformation mechanisms in quartz: The effect of water.
351 Tectonophysics, 27, 271-294.
352 Burns, R.G. (1970) Mineralogical Applications of Crystal Field Theory. 224 p. Cambridge
353 University Press, Great Britain.
354 Carlson, W.D., Gale, J.D., Wright, K. (2014) Incorporation of REEs in aluminosilicate garnet:
355 Energetics from atomistic simulation. American Mineralogist, in press. DOI:
356 10.2138/am.2014.4720.
357 Cherniak, D.J., Watson, E.B., and Wark, D.A. (2007) Ti diffusion in quartz. Chemical Geology,
358 236, 65-74.
359 Dick, B.G., Jr., and Overhauser, A.W. (1958) Theory of the dielectric constants of alkali halide
360 crystals. Physical Review, 112, 90-103.
361 Gale, J.D. (1997) GULP: A computer program for the symmetry-adapted simulations of solids.
362 Faraday Transactions, 93, 629-637.

Gale, J.D., and Rohl, A.L. (2003) The General Utility Lattice Program (GULP). Molecular Simulation, 29, 291-341.

Ghent, E.D., and Stout, M.Z. (1984) $TiO_2$ activity in metamorphosed pelitic and basic rocks: principles and applications to metamorphism in southeastern Canadian Cordillera. Contributions to Mineralogy and Petrology, 86, 248-255.

Grujic, D., Stipp, M., and Wooden, J.L. (2011) Thermometry of quartz mylonites: Importance of dynamic recrystallization of Ti-in-quartz reequilibration. Geochemistry Geophysics Geosystems, 12(6), 1-19.

Gunawardane, R.P., Fletcher, J.G., Dissanayake, M.A.K.L., Howie, R.A., and West, A.R. (1994) Crystal structure refinement of $Li_4TiO_4$ containing tetrahedrally coordinated $Ti^{4+}$ and tetragonally packed oxide ions. Journal of Solid State Chemistry, 112, 70-72.

Hirth, G., and Tullis, J. (1992) Dislocation creep regimes in quartz aggregates. Journal of Structural Geology, 14, 145-159.

Huang, R., and Audétat, A. (2012) The titanium-in-quartz (TitaniQ) thermobarometer: A critical examination and re-calibration. Geochimica et Cosmochimica Acta, DOI: 10.1016/j.gca.2012.01.009, 31.

Kantorovich, L.N. (1995) Thermoelastic properties of perfect crystals with nonprimitive lattices. I. General theory. Physical Review B, 51, 3520-3534.

Kidder, S., Avouac, J.-P., and Chan, Y.-C. (2013) Application of titanium-in-quartz thermobarometry to greenschist facies veins and recrystallized quartzites in the Hsüehshan range, Taiwan. Solid Earth, 4, 1-21.

Lewis, G.V., and Catlow, C.R.A. (1986) Defect studies of doped and undoped Barium Titanate using computer simulation techniques. Journal of Physics and Chemistry of Solids, 47(1), 89-97.

Mott, N.F., and Littleton, M.J. (1938) Conduction in polar crystals. I. Electrolytic conduction in solid salts. Transactions of the Faraday Society, 34, 485-499.

Müller, A., Wiedenbeck, M., Van Den Kerkhof, A.M., Kronz, A., and Simon, K. (2003) Trace elements in quartz - a combined electron microprobe, secondary ion mass spectrometry, laser-ablation ICP-MS, and cathodoluminescence study. European Journal of Mineralogy, 15, 747-763.

Nachlas, W.O., Hirth, G., Teyssier, C., Whitney, D.L., and Zimmermann, M. (2013) Synthesis and deformation of a Ti doped quartz aggregate. EGU General Assembly, EGU2013-9892.

Pauling, L. (1980) The nature of silicon-oxygen bonds. American Mineralogist, 65, 321-323.

Purton, J.A., Allan, N.L., Blundy, J., and Wasserman, E.A. (1996) Isovalent trace element partitioning between minerals and melts — a computer simulation model. Geochimica et Cosmochimica Acta, 60, 4977-4987.

Raz, U., Girsperger, S., and Thompson, A.B. (2002) Thermal expansion, compressibility and volumetric changes of quartz obtained by single crystal dilatometry to 700 $^{o}$C and 3.5 kilobars (0.35 GPa). Schweizerische Mineralogische und Petrographische Mitteihurgen 83, 173-182.

Rusk, B.G., Lowers, H.A., and Reed, M.H. (2008) Trace elements in hydrothermal quartz: Relationships to cathodoluminescent textures and insights into vein formation. Geology, 36(7), 547-550.

Rusk, B.G., Reed, M.H., Dilles, J.H., and Kent, A.J.R. (2006) Intensity of quartz cathodoluminescence and trace-element content in quartz from the porphyry copper deposit at Butte, Montana. American Mineralogist, 91, 1,300-1,312.

Sanders, M.J., Leslie, M., and Catlow, C.R.A. (1984) Interatomic potentials for $SiO_2$. Journal of the Chemical Society, Chemical Communications, 1271-1273.

Spear, F.S., and Wark, D.A. (2009) Cathodoluminescence imaging and titanium thermometry in metamorphic quartz. Journal of Metamorphic Geology, 27, 187-205.

Taylor, M.B., Barrera, G.D., Allan N.L., Barron, T.H.K., and Mackrodt W.C. (1997) Free energy of formation of defects in polar solids. Faraday Discussions, 106, 377-387.

Thomas, J.B. (2013) Experimental calibration of a Ti-in-quartz thermobarometer: An overview for applications to mylonites. EGU General Assembly Conference Abstracts, 15, p. 8555.

Thomas, J.B., Watson, E.B., Spear, F.S., Shemella, P.T., Nayak, S.K., and Lanzirotti, A. (2010) TitaniQ under pressure: The effect of pressure and temperature on the solubility of Ti in quartz. Contributions to Mineralogy and Petrology, 160(5), 743-759.

Wark, D.A., and Spear, F.S. (2005) Titanium in quartz: Cathodoluminescence and thermometry. Geochimica et Cosmochimica Acta Supplement, 69, A592.

Wark, D.A., and Watson, E.B. (2006) TitaniQ: A titanium-in-quartz geothermometer. Contributions to Mineralogy and Petrology, 152, 743-754.

426 ## FIGURE CAPTIONS

427

428 **Figure 1.** Calculated lattice energy for supercells of varying dimension, each containing a single
429 Ti cation substituting for Si. Small supercells contain high [Ti] and yield elevated lattice
430 energies due to interactions among closely spaced defects; however, at lower
431 concentrations, with Ti cations separated by > ~30 Å or more, this energy perturbation is
432 negligible.

433

434 **Figure 2.** CL imaging for Ti distribution analysis in quartz mylonites from: (a,b) Ashley et al.
435 (2013); (c) Grujic et al. (2011); (d) Kidder et al. (2013). (a) Ti equilibration during quartz
436 growth events has aided in reconstructing prograde and early retrograde *P-T-D* histories
437 in quartz tectonites (Ashley et al., 2013). However, in dynamically recrystallized quartz,
438 subgrains typically contain lower [Ti] than relict porphyroclastic cores (appearing darker
439 in CL images; b-d). These Ti-deficient grains result in temperature estimates much lower
440 than those produced by other thermobarometric techniques.

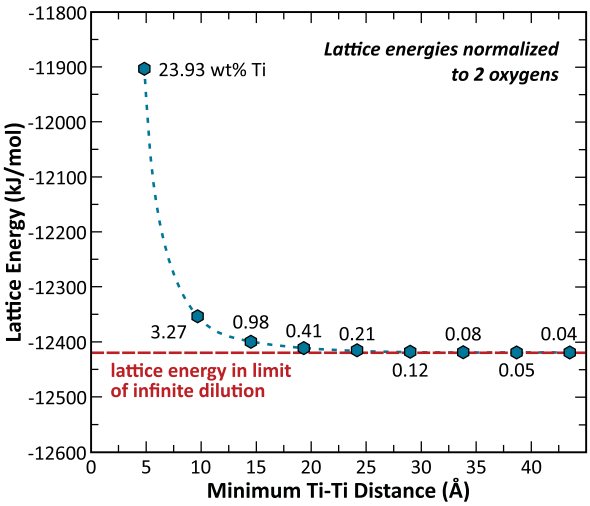
Lattice energies normalized
to 2 oxygens
23.93 wt% Ti
3.27
0.98
0.41
0.21
0.12
0.08
0.05
0.04
lattice energy in limit
of infinite dilution
Lattice Energy (kJ/mol)
-11800
-11900
-12000
-12100
-12200
-12300
-12400
-12500
-12600
0
5
10
15
20
25
30
35
40
Minimum Ti-Ti Distance (Å)

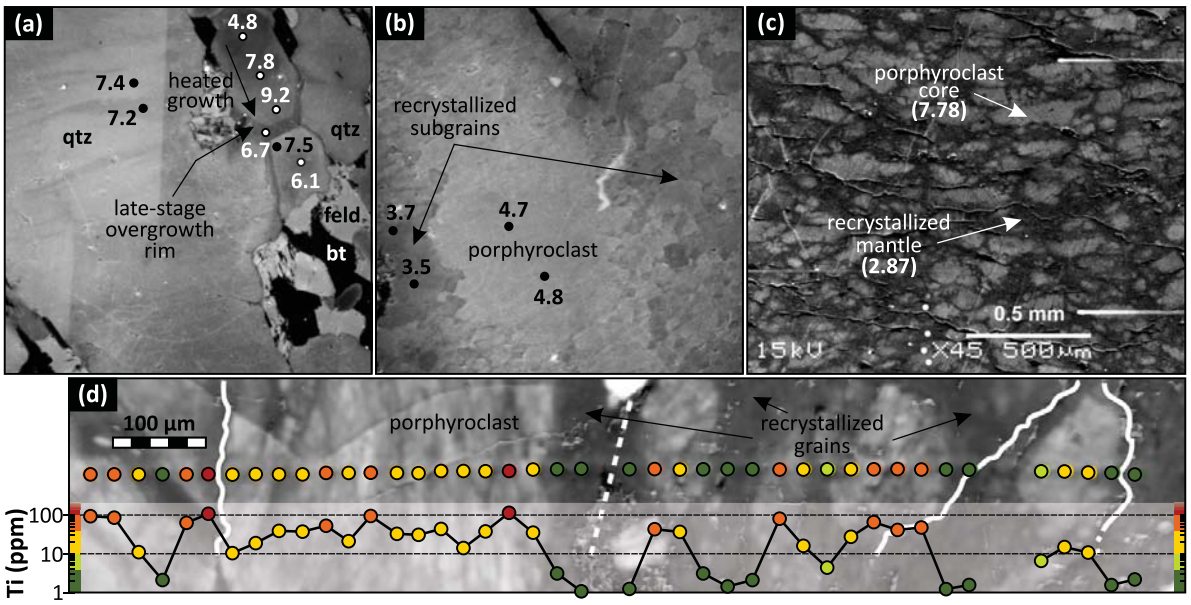
(a)
4.8
7.8
7.4
heated
growth
9.2
7.2
qtz
qtz
6.7
7.5
6.1
late-stage
overgrowth
rim
feld
bt
(b)
recrystallized
subgrains
3.7
4.7
porphyroclast
3.5
4.8
(c)
porphyroclast
core
(7.78)
recrystallized
mantle
(2.87)
0.5 mm
15kV
X45 500µm
(d)
100 µm
porphyroclast
recrystallized
grains
Ti (ppm)
100
10
1

**Table 1.** Parameters for interatomic potentials

| Interaction | *A* (kJ·mol$^{-1}$) | ρ (Å) | *C* (kJ·mol$^{-1}$·Å$^{-6}$) | Source |
|---|---|---|---|---|
| $Si^{4+}$ $O^{2-}$ | 123878 | 0.3205 | 1028 | 1 |
| $Ti^{4+}$ $O^{2-}$ | 84637 | 0.3810 | 868 | 2 |
| $O^{2-}$ $O^{2-}$ | 2196384 | 0.1490 | 2690 | 1 |
| **Interaction** | **Shell charge (\|e\|)** | | ***k*** **(kJ·mol$^{-1}$·Å$^{-2}$)** | **Source** |
| $O^{2-}$ (core-shell) | -2.86902 | | 7229 | 3, 1 |
| **Interaction** | **$K_B$ (kJ·mol$^{-1}$·rad$^{-2}$)** | | **$\theta_0$ (°)** | **Source** |
| $O^{2-}$ $Si^{4+}$ $O^{2-}$ | 2.097 | | 109.47 | 1 |

*Notes:* All short-range interactions for $O^{2-}$ act on the shell of the ion. The cut-off distance for the $Si^{4+}$ $O^{2-}$ and $Ti^{4+}$ $O^{2-}$ Buckingham potentials was 12 Å.

*Sources: 1 - Sanders et al. (1984); 2 - Lewis and Catlow (1986); 3 - Purton et al. (1996).*

**Table 2.** Lattice energies (per 2 oxygens) of α-quartz supercells with single Ti substitution

| Supercell dim. | No. of unit cells | Supercell comp. Ti | Si | O | [Ti] (ppm) | [Ti] (wt. %) | Min. Ti-Ti dist. (Å) | Lattice Energy ($kJ \cdot mol^{-1}$) |
|---|---|---|---|---|---|---|---|---|
| 1x1x1 | 1 | 1 | 2 | 6 | 239290 | 23.93 | 4.835 | -11903.74 |
| 2x2x2 | 8 | 1 | 23 | 48 | 32744 | 3.27 | 9.669 | -12352.89 |
| 3x3x3 | 27 | 1 | 80 | 162 | 9795 | 0.98 | 14.504 | -12399.40 |
| 4x4x4 | 64 | 1 | 191 | 384 | 4142 | 0.41 | 19.339 | -12410.74 |
| 5x5x5 | 125 | 1 | 374 | 750 | 2123 | 0.21 | 24.174 | -12414.77 |
| 6x6x6 | 216 | 1 | 647 | 1296 | 1229 | 0.12 | 29.008 | -12416.56 |
| 7x7x7 | 343 | 1 | 1028 | 2058 | 774 | 0.08 | 33.843 | -12417.47 |
| 8x8x8 | 512 | 1 | 1535 | 3072 | 519 | 0.05 | 38.678 | -12417.98 |
| 9x9x9 | 729 | 1 | 2186 | 4374 | 364 | 0.04 | 43.512 | -12418.28 |

*Abbreviations: dim. – dimensions; no. – number; comp. – composition; min. – minimum; dist. – distance.*